

Wright State University

CORE Scholar

---

Physics Faculty Publications

Physics

---

9-1-1989

## Silicon Crystallite formation in Ion-Implanted Quartz

U. B. Ramabadran

H. E. Jackson

Gary C. Farlow

Wright State University - Main Campus, gary.farlow@wright.edu

Follow this and additional works at: <https://corescholar.libraries.wright.edu/physics>



Part of the [Physics Commons](#)

---

### Repository Citation

Ramabadran, U. B., Jackson, H. E., & Farlow, G. C. (1989). Silicon Crystallite formation in Ion-Implanted Quartz. *Applied Physics Letters*, 55 (12), 1199-1201.  
<https://corescholar.libraries.wright.edu/physics/35>

This Article is brought to you for free and open access by the Physics at CORE Scholar. It has been accepted for inclusion in Physics Faculty Publications by an authorized administrator of CORE Scholar. For more information, please contact [library-corescholar@wright.edu](mailto:library-corescholar@wright.edu).

# Silicon crystallite formation in ion-implanted quartz

Uma B. Ramabadran and Howard E. Jackson  
*Department of Physics, University of Cincinnati, Cincinnati, Ohio 45221*

G. C. Farlow  
*Department of Physics, Wright State University, Dayton, Ohio 45435*

(Received 12 April 1989; accepted for publication 10 July 1989)

Rapid thermally annealed silicon-implanted  $x$ -cut  $\alpha$ -quartz samples have been examined by Rutherford backscattering and Raman microprobe spectroscopy. The data indicate that the silicon has diffused at 1200 °C to form a buried layer of crystallites of size 1–10  $\mu\text{m}$ . The crystallites are preferentially oriented and under substantial stress.

A powerful method of modifying local properties in semiconductors and insulators is ion implantation. In addition to the widely used controlled doping of semiconductors, it can be used to form buried insulating layers by implantation of oxygen or nitrogen in silicon and subsequently inducing a thermally activated chemical reaction (SIMOX structures).<sup>1,2</sup> Recently, ion implantation of Sb, P, Ge, and As into thermally grown amorphous  $\text{SiO}_2$  has provided evidence for the precipitation of these dopants into clusters upon heating.<sup>3</sup> The ion implantation of silicon into amorphous quartz and subsequent thermal processing by laser annealing or rapid thermal annealing (RTA) has also recently been investigated.<sup>4</sup> Depending on the annealing conditions, silicon migration towards or away from the surface of the sample may occur. In order to investigate the behavior of silicon ion implanted into crystalline quartz, we have used high implant doses followed by rapid thermal annealing at a temperature of 1200 °C. We show that a buried layer of silicon islands with an average size of several microns is formed after rapid thermal annealing and that the silicon formed is crystalline, under substantial stress, and preferentially oriented.

The samples were prepared by implanting unpolished samples of  $x$ -cut  $\alpha$ -quartz with Si. The implantation energy of 150 keV and the dose of  $4 \times 10^{17} \text{ cm}^{-2}$  were chosen so that the density of excess Si between 120 and 250 nm below the surface would approach that of elemental Si. Identically implanted samples were thermally annealed under three different conditions. Sample A was rapid thermally annealed at 1200 °C for 2 min with a slow ramp (2 min) in an argon atmosphere. Sample B underwent a relatively fast ramp up, remained at 500 °C for 2 min, and was annealed for 2 min at 1200 °C, all in an argon atmosphere. Sample C underwent a furnace anneal at 1000 °C for 1 h in a flowing nitrogen atmosphere.

In Fig. 1 we display a differential interference optical micrograph of sample A after thermal annealing. We observe dark regions which are identified later as silicon regions. These regions are several microns in size and extend over the whole surface of the sample. A similar optical micrograph of sample B, which underwent a somewhat faster rapid thermal anneal, also shows aggregates of Si. The Si regions are typically smaller in size and less connected than for sample A. A high magnification micrograph of the furnace-annealed sample reveals a relatively uniform distribu-

tion of even smaller isolated silicon regions about 1  $\mu\text{m}$  in size.

Rutherford backscattering (RBS) was used to determine the depth distribution and stoichiometry of the implanted silicon. The RBS was taken using a 2 MeV  $\text{He}^+$  beam with 160° backscattering angle and 45° tilt angle. This geometry provides a depth resolution of approximately 7.5 nm and stoichiometries to within 10%. Figure 2(a) shows the backscattered yield plotted against the energy of backscattered He ions from both the implanted and unimplanted regions of the unannealed sample. The increase in yield at 1.18 MeV in the spectrum is characteristic of silicon, while that at 0.76 MeV is characteristic of oxygen.<sup>5</sup> The difference in yield between the RBS spectra in the energy range from 0.90 to 1.18 MeV is a measure of the number of silicon ions implanted into the  $\text{SiO}_2$  substrate. The difference per unit area between the yields of the spectra in the 0.50–0.76 MeV range reflects the nature of change in the oxygen stoichiometry of the implanted region of the substrate. A depth scale appropriate to stoichiometric  $\text{SiO}_2$  is indicated for the silicon backscattered yields. The data indicate that the implanted silicon is distributed from the surface to about 350 nm with a peak at a depth of about 200 nm. The measured integrated dose is about  $2 \times 10^{17} \text{ cm}^{-2}$  which is less than the  $4 \times 10^{17} \text{ cm}^{-2}$  inferred from charge integration during implantation.

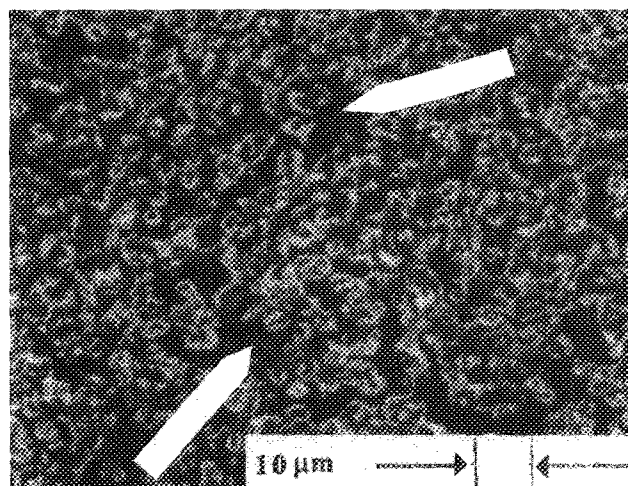


FIG. 1. Optical micrograph of RTA sample A with the arrows pointing to examples of silicon regions (dark regions in this micrograph).

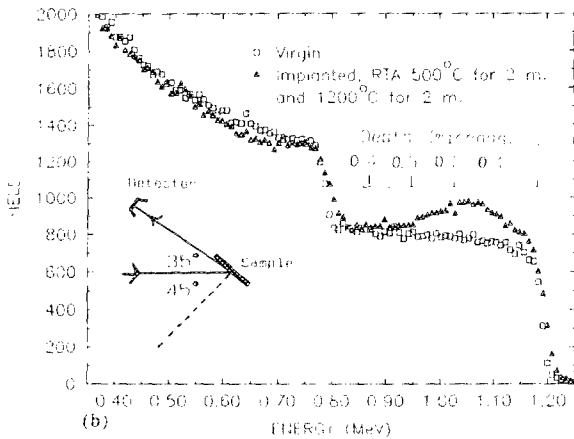
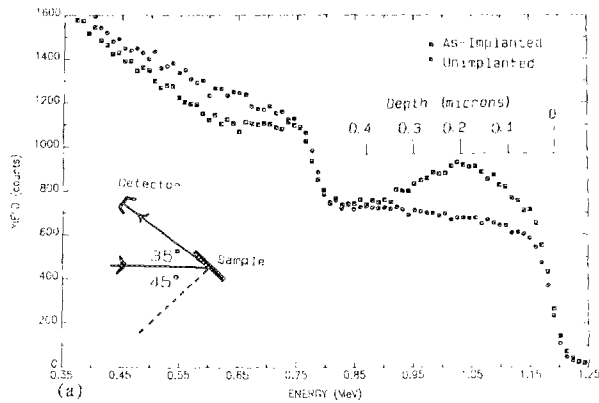


FIG. 2. Rutherford backscattering spectra indicating excess silicon at a depth of about 200 nm: (a) as-implanted, unannealed sample; (b) RTA sample B.

The retained dose ( $2 \times 10^{17} \text{ cm}^{-2}$ ) reflects sputtering which is typical of high-dose implantation in high vacuum. The average concentration near the peak is approximately  $3.5 \times 10^{22} \text{ cm}^{-3}$ , which compares with  $2.3 \times 10^{22} \text{ cm}^{-3}$  for stoichiometric  $\text{SiO}_2$  and  $5 \times 10^{22} \text{ cm}^{-3}$  for elemental silicon.

The RBS obtained after the rapid thermal annealing (sample B) are displayed in Fig. 2(b) and may be compared to similar spectra from unimplanted  $\text{SiO}_2$ . We observe that the silicon bearing layer remains buried at the initial implanted depth; there is no evidence of diffusion into the bulk nor segregation to the surface. The average concentration near the peak for sample B is about  $3.3 \times 10^{22} \text{ cm}^{-3}$ , which is not significantly different from the as-implanted concentration. The distribution of excess silicon remains essentially the same as is found in the as-implanted samples. The RBS performed on the nitrogen-annealed sample C shows a silicon distribution similar to that observed in the other samples.

Raman microprobe spectroscopy with a spatial resolution of  $1 \mu\text{m}$  was used to investigate the possible formation of microcrystals in the implanted sample. Laser light of wavelength 514.5 nm at a typical power of 5 mW was used. Raman spectra taken from the as-implanted sample showed a broadband centered roughly around  $450 \text{ cm}^{-1}$  characteristic of amorphous quartz.<sup>6</sup> Phonons at energies of 464 and  $509 \text{ cm}^{-1}$  expected in crystalline quartz<sup>7</sup> were not observed. From this we conclude that the quartz was disordered dur-

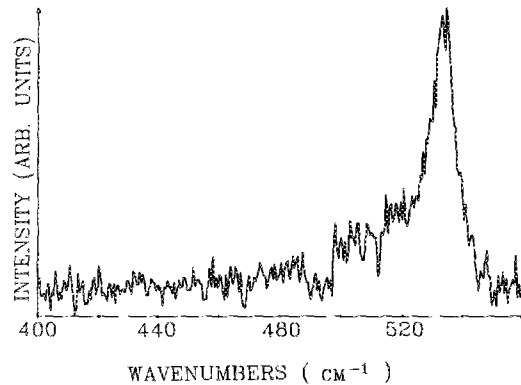


FIG. 3. Raman spectrum of RTA sample A with the quartz peaks removed showing a crystalline silicon signature at  $526.5 \text{ cm}^{-1}$ .

ing implantation; no evidence of elemental silicon was observed in this spectrum. Following rapid thermal annealing, the Raman spectra of crystalline quartz were recovered with evidence of an additional peak, discussed below. No evidence of remaining disordered quartz was observed.

Raman data from the rapid thermally annealed sample A are displayed in Fig. 3. This spectrum was obtained by subtracting a spectrum taken from a similarly annealed crystalline quartz from a spectrum taken from the silicon-rich region. The peak at  $526.5 \text{ cm}^{-1}$  may be compared to the longitudinal optic Raman peak of crystalline Si at  $522.5 \text{ cm}^{-1}$ .<sup>8</sup> The observed shift indicates that a compressive stress of about  $10^{10} \text{ dyn/cm}^2$  is experienced by the silicon crystallites.<sup>9</sup> The linewidths of the longitudinal optic peak of silicon were about  $11 \text{ cm}^{-1}$  and may reflect both finite grain size<sup>9</sup> and inhomogeneous strain. No variations in the frequencies of the quartz peaks were observed indicating that the stress observed for the silicon microcrystals is not generally experienced by the substrate. Rapid thermally annealed sample B provided similar results, i.e., an  $11 \text{ cm}^{-1}$  linewidth and a peak position of  $526.5 \text{ cm}^{-1}$ . Polarized Raman data from several crystallites are consistent with a  $\langle 111 \rangle$  silicon orientation parallel to the  $x$  axis of the quartz crystal.

In summary, we have demonstrated that microcrystalline silicon of several microns in diameter forms below the surface of silicon implanted, rapid thermally annealed  $x$ -cut  $\alpha$ -quartz. The silicon forms larger areas for a slower RTA process than for either a faster RTA process or a furnace anneal; each process proceeds at a temperature between 1000 and  $1200 \text{ }^\circ\text{C}$ . Preliminary polarized Raman experiments suggest a preferred direction of silicon crystal formation. The crystalline silicon formed is under substantial stress and is distributed between 100 and 300 nm below the surface.

The authors wish to acknowledge use of the Surface Modification and Characterization Facility operated by Martin Marietta Energy Systems, Inc., for the Division of Materials Science, U.S. Department of Energy under contract No. DE-AC05-84OR21400.

<sup>1</sup>S. T. Davey, J. R. Davis, K. J. Reeson, and P. L. F. Hemment, *Appl. Phys. Lett.* 52, 465 (1988).

<sup>2</sup>R. F. Pinizzotto, *MRS Proc.* **27**, 265 (1984).

<sup>3</sup>G. K. Celler, L. E. Trimble, T. T. Sheng, S. G. Kosinski, and K. W. West, *Appl. Phys. Lett.* **53**, 1178 (1988).

<sup>4</sup>Tsutomu Shimizu, Noriaki Itoh, and Noriaki Matsunami, *J. Appl. Phys.* **64**, 3663 (1988).

<sup>5</sup>W. K. Chu, J. W. Mayer, and M. A. Nicolet, *Backscattering Spectrometry*

(Academic, New York, 1978).

<sup>6</sup>R. Tsu, J. Gonzalez-Hernandez, J. Dohler, and S. R. Ovshinsky, *Solid State Commun.* **46**, 79 (1983).

<sup>7</sup>J. F. Scott and S. P. S. Porto, *Phys. Rev.* **161**, 903 (1967).

<sup>8</sup>Paul A. Temple and C. E. Hathaway, *Phys. Rev. B* **7**, 3685 (1973).

<sup>9</sup>I. H. Campbell and P. M. Fauchet, *Solid State Commun.* **58**, 739 (1986).